

Anode-Supported Solid Oxide Fuel Cells with Thin Film Electrolyte for Operation at Reduced Temperatures

Haiming Xiao* and Thomas Reitz**

**Aerospace Power and Propulsion, UES Corp.
Dayton, Ohio 45432-1894, USA*

***Propulsion Directorate, Air Force Research Laboratory
Wright-Patterson AFB, Ohio 45433-7251, USA*

ABSTRACT

In order to reduce the operating temperature of solid oxide fuel cells (SOFCs), anode-supported cells incorporating thin film (~10 μm) electrolytes in conjunction with anode/electrolyte and cathode/electrolyte interlayers were studied. Anode supported button cells were prepared through a conventional approach and were analyzed via Scanning Electron Microscopy (SEM), Polarization, and Electrochemical Impedance Spectroscopy (EIS). It was found that the electro-catalytic activity and electrode/electrolyte interfacial areas were enhanced through the addition of these interlayers. This performance improvement was attributed to the introduction of a diffuse mixed conduction region associated with these interlayers. The cathode appeared to benefit disproportionately from this enhancement.

INTRODUCTION

Solid oxide fuel cells (SOFCs) are energy conversion devices that produce electricity by electrochemically combining reactions of fuel and oxidant gases across an ionic-conducting ceramic. SOFCs are anticipated to become very competitive devices for electrical power generation because of their high efficiency and lower pollution potential. SOFCs are an attractive option relative to polymer electrolyte fuel cells because they exhibit greater fuel tolerance, higher efficiencies, and produce high-grade waste heat making them suitable for combined heat and power applications. SOFCs are reaching pre-commercialization with several hundreds of residential stationary power units (about 1 kW) being tested and larger units (250 kW or above) being evaluated by various utility companies world wide [1-2]. Although great progresses have been made, at present the SOFC technology is still in its development (or pre-commercialization) stage and several technical challenges remain to be solved before it becomes a practical power system.

In conventional SOFCs, the electrolyte is yttria-stabilized zirconia (YSZ) with thickness of ~200 μm , and the operating temperature is around 900-1000°C. These high operating temperatures place considerable constraints on materials which can be used for interconnections and construction (manifold parts and seals etc.). Because these materials are often cost prohibitive, lowering the operation temperature is critical for ensuring SOFC's cost effectiveness. In order to achieve these temperature decreases, many researchers have explored the use of thin film electrolytes with high degrees of

success [3-5]. While these thin film electrolytes do enable operation at lower temperature, activation polarization, especially on the cathode are significantly more pronounced under these conditions. Others have explored the application of thin film composite interlayers as a means to improve charge transfer reaction in the electrode/electrolyte interface for both anode and cathode [6,7]. The nature of these interlayers is still a matter of contention and further studies are required to adequately understand their function. The objective of this effort is to examine the performance of thin film, anode-supported SOFCs when anode and cathode interlayers are used to enhance the anode/electrolyte and cathode/electrolyte interfaces. Electrochemical Impedance Spectroscopy is used to generate a more complete understanding of how these interfaces improve cell performance.

EXPERIMENTAL

Cell fabrication

Test cells were generally constructed through a five layer process which includes: (a) porous Ni+YSZ anode support; (b) anode/electrolyte interlayer; (c) dense YSZ electrolyte; (d) cathode/electrolyte interlayer; (e) porous LSM (LaSrMnO_3) cathode current collector. An objective of this study was to evaluate the impact of a thin film layer which acts to transition the structural and conducting properties from electrolyte to electrode. Typical interlayer compositions were employed in this study in order to increase the applicability of the results. Their composition was 50%YSZ-50%LSM for cathode/electrolyte and 50%YSZ-50%NiO for anode/electrolyte interlayer. The cell fabrication process is briefed as follows: NiO and YSZ materials were purchased from commercial sources and mixed in requisite proportions then ball milled with measured amounts of rice flour or carbon to induce porosity. The mixed powders then were uniaxially die-pressed into discs of ~ 3.3 cm in diameter and ~ 1.2 mm of thickness. Colloidal slurries of anode/electrolyte interlayer and electrolyte were sequentially sprayed on the anode discs. The coated discs were sintered in air at 1400°C at a controlled rate. Cathode interlayer and LSM cathode slurries were applied onto the half cells respectively to make completed button cells. The cathode surface area (A) was controlled to a known value so that current density can be calculated for electrochemical measurements. A completed view of the anode supported button cell is presented in Figure 1.

Cell testing

Four probe voltage and current measurements were accomplished by attaching two platinum, silver, or gold leads to the anode and cathode. The anode supported cell was sealed onto an alumina tube (Vesuvius) with high temperature cement (Cerambond 552, Aremco Products Inc.). A specially-designed quartz fixture for feeding fuel gas and releasing exhaust gas was connected to the alumina tube through a compression fitting (Swagelok). Sealing around the anode leads was accomplished through two treaded bushings with silicon rubber septums (ACE Glass) which were attached to the quartz fixture via a graded seal. The completed cell was then placed into the isothermal zone of a clam-shell furnace. Reduction of the NiO to Ni was achieved through a controlled temperature ramp in an anode flow stream of 10% H_2 , balance N_2 TGA (thermal gravity

analysis) determined that 98% of NiO was reduced by 440 °C in pure hydrogen suggesting that complete reduction of the anode would be achieved by 500 C. No significant difference in cell performance was observed as a function of reduction temperature in the range of 600°C to 800°C. Controlled reduction of NiO is essential to promote high anode conductivity and sufficient porosity. After the anode reduction was complete, the cell was brought to the desired temperature for testing and the reactant gas was switched to humidified hydrogen gas. The cathode chamber is not sealed, so a purified air stream was blown over the surface to ensure ample oxygen availability. Electrochemical characterization was conducted using Solartron 1260 Impedance gain/phase analyzer coupled to a Solartron 1287 Electrochemical Interface. A picture of the completed cell and testing fixture are displayed in Figure 1.

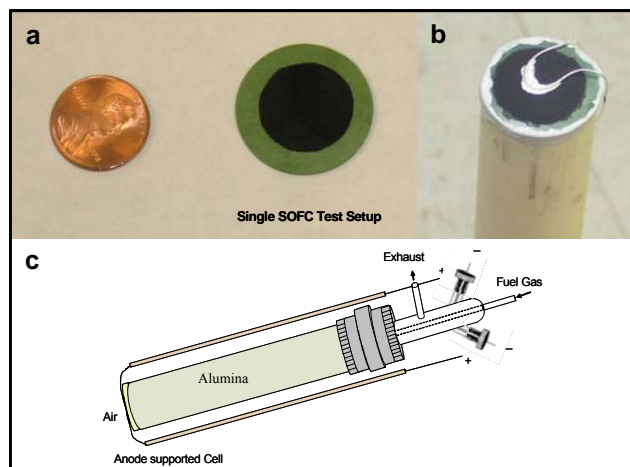


Figure 1: (a) Anode supported button cell, (b) button cell mounted to alumina tube, (c) schematic of cell testing fixture

RESULTS AND DISCUSSION

Scanning electronic microscopy (SEM) was used to characterize the quality of the electrode, interfacial, and electrolyte layers during fuel cell construction. A micrograph for the surface analysis of a typical porous anode is presented in Figure 2-a. Providing sufficient electrode porosity is vital to ensure that concentration polarizations will not manifest at high current densities. However, it is important that a balance is achieved between porosity and structural stability of the electrode support. It has been reported that the introduction of 20% to 45% porosity within the anode substrates provides for ample reactant mobility without compromising structural stability [8]. As discussed earlier, porosity of samples examined under this study were controlled at ~25% through the addition of 10% rice flour or carbon powder during green electrode fabrication.

Figure 2-b presents the micrograph of the dense YSZ electrolyte layer prepared by colloidal spray application onto the porous anode support. It is clear from the figure that no pores are observed potentially indicating that a fully-dense membrane was achieved. Density and continuity of the electrolyte is of critical concern in these cells as even small imperfections in this layer contribute to unacceptably low open circuit voltages. A cross-

sectional view of a complete 5 layer anode button cell is presented as Figure 2-c. This micrograph clearly shows that a dense, continuous electrolyte layer with thickness of $\sim 10\ \mu\text{m}$ was achieved. It is also observed that the neighboring electrodes appear sufficiently porous with a continuous electrode/electrolyte interface.

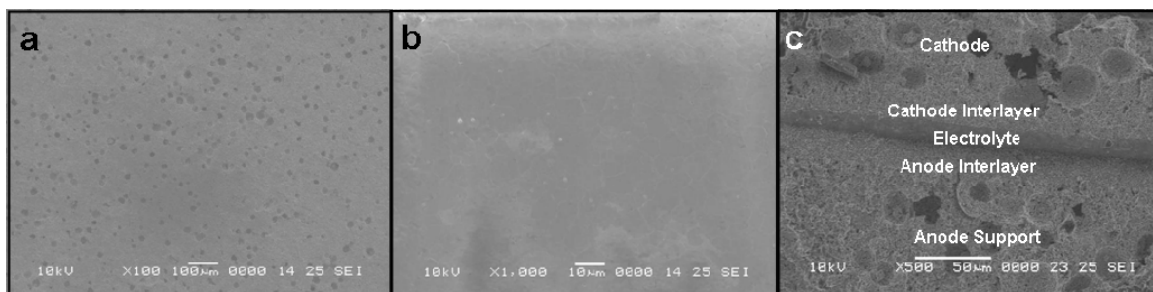


Figure 2. (a) SEM micrograph for surface analysis of a typical porous anode-support before hydrogen reduction (x100) and (b) YSZ electrolyte (x1000), (c) SEM micrograph of a cross-section analysis of a typical anode-supported cell (x500)

Button cells were characterized for performance at various temperature using humidified hydrogen and air as reactants. Samples were brought to temperature and characterized to determine their current-potential and impedance response. Figure 3 demonstrates the stability of the open circuit voltage (OCV) of a typical anode supported cell as a function of time. The OCVs of typical cells examined under this study were in a range from 1.05 V to 1.12 V which is within good agreement with that predicted by the Nernst equation; 1.10 V at 800°C .

OCV reading is an important indicator of cell performance and is indicative of the hermeticity of seal as well as the continuity of the electrolyte layer. It can be readily observed that even a minute defect within the seal or electrolyte layer will result in the observed OCV falling far below the thermodynamically predicted value.

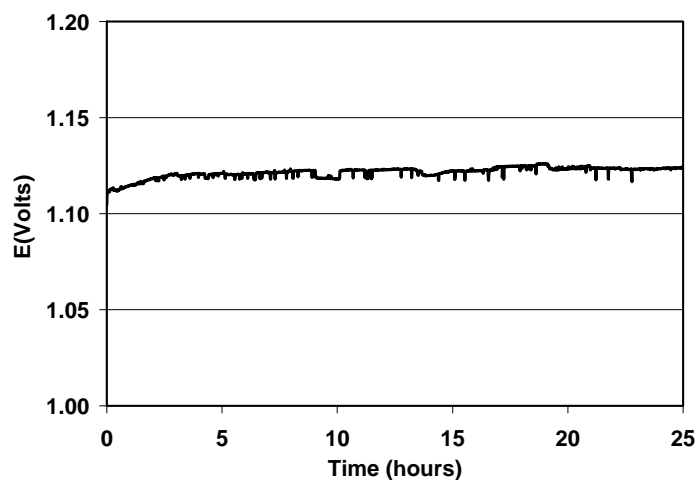


Figure 3: The OCV of a typical 5-layer anode-supported cell as a function of time at 800°C

It has been previously observed that the application of a thin, porous interlayer between the bulk electrode structure and dense electrolyte membrane can significantly increase cell performance. These interlayers typically involve reducing the concentration of active material (e.g. Ni or LSM) while increasing the concentration of support phase (YSZ) in order to induce greater homogeneity with the dense electrolyte membrane. A polarization curve illustrating the impact of this interlayer on a typical fuel cell is presented below (Fig 4). The maximum power density achieved was significantly greater for the specimen containing the thin, interfacial layers. Ohmic resistance was calculated to be $0.26 \Omega\text{-cm}^2$ and $0.81 \Omega\text{-cm}^2$ for the 5-layer and 3-layer assemblies, respectively, using a non-linear, least-squares approach. An OCV of 1.08 V was observed for the 5 layer assembly which is slightly higher than that observed for the 3-layer assembly, ~ 1.00 V. The exact extent to which the introduction of the interlayers impacted the OCV is difficult to determine, however, it was generally observed that their addition did appear to improve the seal integrity. This is attributed to the higher content of YSZ in the interlayer which allows for greater thermal expansion match with the ceramic sealing material. It is difficult to determine the exact reason for the decrease in the area specific resistance for the sample with interlayers. While the specific thicknesses of the electrolytes were not explicitly determined, they were nominally similar for both specimens. It is noted that the high number of processing steps required for cell production will obviously translate into some variability between samples. However, this variability is unlikely to contribute to this extent. Some process improvements did occur as the authors adopted the 5-layer process which probably contributed significantly to the sharp contrast between the samples' ohmic resistances. A poor contact at either current collector could also contribute to this difference. Despite this inconsistency, the data still reveals some insight into the advantages associated with incorporating these interfaces. Overpotentials associated with the cell lacking interlayers appear to be entirely ohmic over the entire current range with no apparent non-linear features occurring at low current densities. This would seem to suggest that reaction kinetics do not appear to be rate controlling for this sample. The sample incorporating the interlayers, by contrast, appears to exhibit a more pronounced decay at lower current densities which would suggest a sharper Tafel slope and greater activation polarization, presumably associated with the cathode.

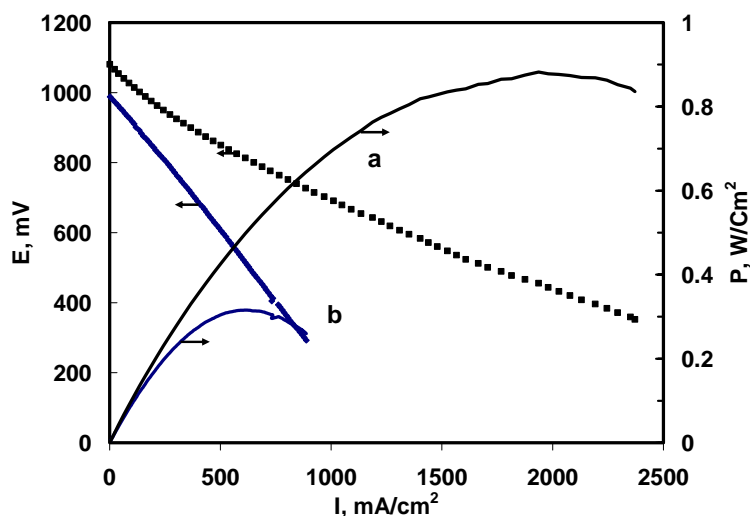


Figure 4: Polarization curve for (a) – anode supported fuel cell incorporating anode and cathode interlayers, (b) - anode supported fuel cell without interlayers, (800°C)

More insight into these differences can be observed by examination of their respective impedance spectra, (Fig 5). Two clear time constants are observed for the 3-layer assembly with the low frequency (<10 Hz) feature appearing significantly more capacitive than the high frequency arc. The low frequency feature was associated with the cathode through variation of gas compositions which is consistent with literature [9]. The 5 layer specimen contains 3 distinct time constants with the predominant feature appearing between the frequencies of 10 to 10^3 Hz. Again, the low frequency feature was assumed to be associated with the cathode. As could be expected through examination of figure 4, the 5-layer specimen exhibits far less total impedance than that observed for the 3-layer.

From examination of these data it appears as though the interlayers increase catalytic activity in the area of three phase (gas/electronic conductor/ionic electrolyte) interface where the charge transfer reactions occur. Because the high frequency features for samples with and without interlayer were not explicitly determined to be associated with a single electrode process, no relative comparison between the anode and cathode impedances could be determined. However, because the oxygen reduction reaction is more sluggish than hydrogen oxidation, it was assumed that the cathode would exhibit a greater enhancement with the addition of the interlayers due to the increase in active area at the interface. A second explanation for this observation is that the LSM cathode is purely an electronic conductor whereas Ni/YSZ anode contributes both electronic and ionic conduction. After introduction of mixed conductive interlayers, the interface of cathode/electrolyte would be expected to be enhanced more substantially than that of anode/electrolyte.

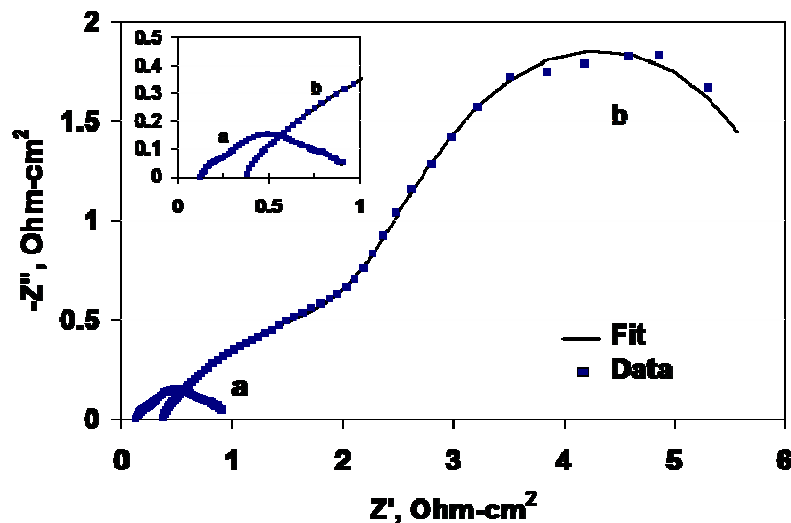
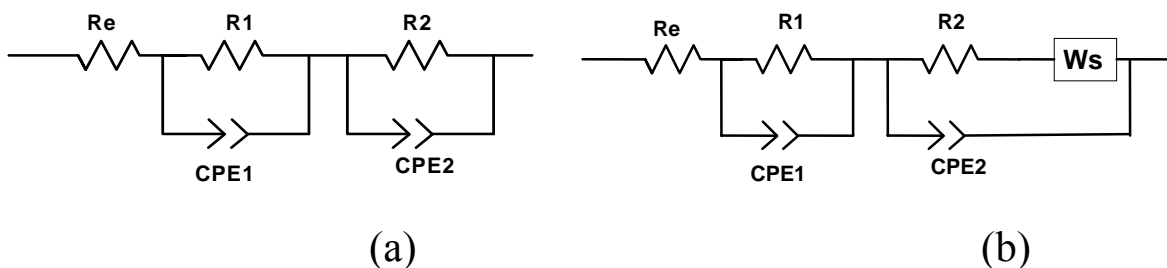


Figure 5: Impedance spectra obtained for single SOFC button cells at 750 °C, (a)-with electrode/electrolyte interlayers, (b)- without electrode/electrolyte interlayers

Model fitting with equivalent circuit diagrams indicate that the cell without interlayer addition (b) is adequately fit to a circuit diagram as shown in figure 6-a, whereas the specimen containing anode and cathode interlayers requires an additional circuit element (Warburg Diffusional Element) in order to be properly represented (6-b). This would

appear to suggest that without electrode/electrolyte interlayers, the area of the interfaces is limited, and charge-transfer reactions at the interfaces are rate-limiting. However, when electrode/electrolyte interlayers are added, the area of the interfaces is significantly increased, accelerating the charge-transfer reactions at the interfaces. Diffusion phenomenon would then be expected to become important, especially at higher current densities. The parameters associated with the circuit models are presented in Table 1.



- R_e Ohmic resistance
 R_1 : High frequency semicircle resistance
 CPE1 High frequency semicircle constant phase element, $Z = 1 / C(i \cdot \omega)^a$
 R_2 : Low Frequency semicircle resistance
 CPE2: Low Frequency semicircle constant phase element
 W_s Warburg element

Figure 6 Equivalent circuits of model fitting with impedance spectra

Table 1 Impedance parameters calculated from model fitting for the cells with electrode/electrolyte interlayers at 750°C

Cells	High Frequency Arc			Low Frequency Arc			
	R_e ($\Omega \cdot \text{cm}^2$)	R_1 ($\Omega \cdot \text{cm}^2$)	CPE_1 ($F \text{ cm}^{-2} \text{ s}^a$)	R_2 ($\Omega \cdot \text{cm}^2$)	CPE_2 ($F \cdot \text{cm}^{-2} \cdot \text{s}^a$)	$W1-R_1$ ($\Omega \cdot \text{cm}^2$)	$W1-T$ ($F \cdot \text{cm}^{-2} \cdot \text{s}^a$)
Without interlayers	0.33	2.64	$C = 0.052$ $a = 0.41$	3.59	$C = 0.13$ * $a = 0.94$		
With Interlayers	0.106	0.82	$C = 0.124$ $a = 0.38$	0.045	$C = 0.005$ * $a = 1.22$		
	0.13	0.10	$C = 0.002$ $a = 0.73$	0.52	$C = 0.026$ $a = 0.64$	0.19	$C = 0.40$ ** $a = 0.36$

* Use Model (a) in Figure 6

** Use Model (b) in Figure 6 where Warburg diffusion was considered.

CONCLUSIONS

The inclusion of interfacial electrode layers on the fuel cell electrodes significantly improved the performance of anode supported cells. Specimens without an interlayer (3-layer) exhibited far greater ohmic resistance than the 5-layer specimen. The extent of mass transfer limitations for the 3-layer specimen could not be readily determined. The inclusion of Warburg term improved the model fit for the 5-layer data suggesting the appearance of mass transfer limitations with the addition of the interlayers. However, the 5-layer specimen exhibited a more pronounced reduction in the charge transfer resistance relative to the 3-layer specimen which is likely why mass transfer resistance became noticeable. Activation polarization was observable in the 5-layer sample at high current densities. Additionally, the open circuit voltage (OCV) was lower for the 3-layer specimen attesting to increased difficulty associated with generating a hermetic seal in these specimens. Impedance spectra illustrated that the cathode for the 3-layer specimen exhibited considerable double layer capacitance and charge transfer resistance which was nearly absent for the 5-layer specimen (anode/cathode interlayer). Incorporating the interfacial layers decreases these impedances largely by introduction of the diffuse mixed conduction region at the electrode/electrolyte interface. Because the bulk cathode material, LSM is predominately an electron conductor, this behavior is especially apparent at the cathode.

REFERENCES

1. S. Colson-Inam, *Fuel Cell Today*, **1**, 1 (2004)
2. J. Larminie and A. Dicks, *Fuel Cell Systems Explained*, John Wiley & Sons Ltd., West Sussex (2003)
3. J.W. Kim, A.V. Virkar, K.Z. Fung, K. Mehta, S.C. Singhal, *J Electrochem Soc*, 146, pp. 69-78 (1999)
4. S. De Souza, S. J. Visco, J.C. DeJonghe, *J Electrochem Soc.*, 144, pp A788-94 (2001)
5. Y.J. Leng, S.H. Chan, K.A. Khor, S.P.Jiang, *Internat. J. of Hydrogen Energy*, 29, pp. 1025-1033 (2004)
6. J.D. Kim, G.D. Kim, J.W. Moon, Y.I Park, W.H. Lee, K. Kobayashi, M. Nagai, C.E. Kim, *Solid State Ionics*, 143, pp. 379-389 (2001)
7. M.J. Jorgenson, S. Primdahl, C. Bagger, M. Mogesen, *Solid State Ionics*, 139, pp. 1-11 (2001)
8. F. Zhao, T. J. Armstrong and A. Virkar., *J. Electrochem. Soc.* **150**, A249 (2003)
9. N. Wagner, W.Schnurnberger, B. Muller, and M. Lang, *Electrochimica Acta*, Vol. 43, No. 24, pp. 3785-3793 (1998)